International Journal of Power Electronics and Drive System (IJPEDS)
Vol. 17, No. 3, September 2026, pp. 1873~1884
ISSN: 2088-8694, DOI: 10.11591/ijpeds.v17.i3.pp1873-1884

Design of PI and fuzzy-based sliding mode controller for speed control of BLDC motor using Landsman converter in electric vehicles

S. Sahana, K. Sasikala
Department of Electrical and Electronics Engineering, Vels Institute of Science, Technology and Advanced Studies (VISTAS), Chennai, India

Article Info

Article history:

Received Oct 8, 2025
Revised May 6, 2026
Accepted Jul 8, 2026

Keywords:

BLDC motor
Fuzzy-based SMC
Landsman converter
PI controller
Sliding mode control

ABSTRACT

This research paper compares a conventional proportional–integral (PI) controller with a fuzzy-based sliding mode controller (FSMC) for speed control of a brushless DC (BLDC) motor powered by a Landsman DC–DC converter for electric vehicle (EV) applications. MATLAB/Simulink is used to model and simulate the proposed system's cascaded control architecture, which consists of a voltage source inverter and a Landsman converter. The performance is assessed in steady-state, load-disturbance, and transient scenarios. According to simulation data, the FSMC outperforms the PI controller in terms of rise time (0.064 s), overshoot (0.17%), and settling time (0.212 s). The FSMC exhibits better resilience, limiting the speed reduction to 45 RPM with a recovery time of 0.04 s with a sudden load disturbance of 1 Nm. The findings verify that the FSMC is appropriate for high-performance BLDC motor drive systems in electric vehicle applications because it provides improved dynamic response and disturbance rejection.

Corresponding Author:

S. Sahana
Department of Electrical and Electronics Engineering
Vels Institute of Science Technology and Advanced Studies (VISTAS)
Chennai, India
Email: sahana.mee05@gmail.com

1. INTRODUCTION

The brushless DC (BLDC) motors are well known for being the best option for electric vehicle (EV) applications because of their great durability, power density, and efficiency. In contrast to traditional brushed DC motors, BLDC motors use electronic commutation instead of brushes, which increase noise, friction, and mechanical wear. EVs can achieve up to 90% efficiency thanks to this feature, which greatly increases their driving range between charges. Additionally, its high power-to-weight ratio facilitates lightweight and compact motor designs, lowering the total weight of the vehicle while enhancing performance. Because BLDC motors don't have brushes, they require less maintenance and have a longer operating life, which makes them a dependable and affordable option for EV applications. Furthermore, their outstanding torque characteristics, which include a high beginning torque and a steady torque across a broad speed range, enable reliable performance and smooth acceleration under a variety of road conditions [1]-[5]. For BLDC motors in EVs to operate effectively and safely, precise speed control is crucial. For smooth and reliable operation, the motor, which serves as the main source of propulsion, must precisely react to driver inputs including acceleration, cruising, and deceleration. By recovering kinetic energy during deceleration, it also increases driving range, maximizes energy efficiency, and permits regenerative braking. Additionally, speed control ensures vehicle stability under a variety of circumstances by supporting safety systems like traction control and anti-lock braking [6]-[8].

The BLDC motors are frequently utilized in automotive and industrial settings because of their effectiveness, portability, and low maintenance requirements. Precise control over torque and speed is still difficult to achieve, though. Despite being widely utilized, proportional-integral (PI) controllers perform poorly when parameters are changed or disturbed. Although sturdy, sliding mode control (SMC) has chattering. By combining fuzzy logic with SMC, the fuzzy sliding mode controller (FSMC) reduces chattering while preserving robustness by adaptively adjusting the switching gain. This work uses a Landsman converter to compare PI and FSMC controllers for a BLDC motor drive [9]-[11]. By offering a steady and controlled DC supply, the Landsman converter successfully reduces voltage swings and ripple from the rectified AC input, improving the performance of BLDC motors. This guarantees a steady DC bus for the inverter, allowing for precise control signal generation, better speed control, less torque ripple, and increased overall performance. It also improves power quality by lowering harmonic distortion. While earlier research has looked at PI, fuzzy, and sliding mode control strategies, the majority either concentrate on traditional DC-DC converters or handle sophisticated converters and intelligent controllers separately. There is still little integrated use of a Landsman converter with a fuzzy sliding mode controller (FSMC), especially in dynamic EV operation environments. In order to close this gap, this paper compares PI and FSMC controllers for a BLDC motor fed by a Landsman converter, with a focus on transient response, disturbance rejection, and applicability for EV applications.

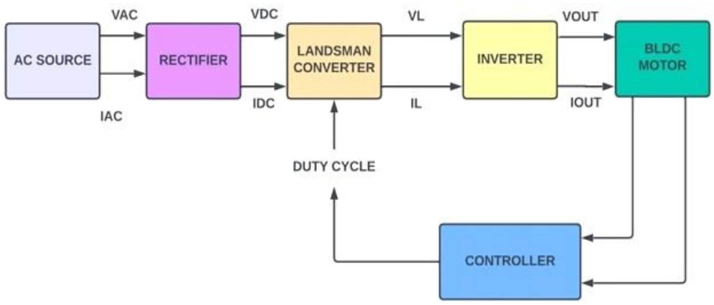

Figure 1. Overall block diagram of the speed control of BLDC motor

2. SYSTEM AND CONVERTER DESIGN

The proposed BLDC motor driving system has a hierarchical control design. To create a DC input, the single-phase AC supply is first rectified and filtered. A Landsman DC–DC converter is then used to control this voltage in order to preserve a stable DC-link under various input and load circumstances. The BLDC motor is powered by a voltage source inverter (VSI) that receives the regulated DC. A cascaded control technique is used, in which the outer loop uses speed error to generate the reference DC voltage while the inner loop controls the converter duty cycle. Accurate speed tracking and strong disturbance rejection are guaranteed by the speed controller, which is built using either a PI or a fuzzy-based sliding mode controller. Figure 1 shows the overall configuration of the system.

2.1. Motor specifications

The BLDC motor used in this simulation has a rated output of 1.2 kW at 48 V. This grade is justified since it represents a conventional, high-power BLDC motor designed for industrial usage. The 48 V rating is widely utilised in commercial and industrial applications, providing a suitable blend of high-power output and safe operating voltage. This approach enables a direct and appropriate comparison of the controllers' performance under normal operating settings. Table 1 shows the specifications of the BLDC motor rating.

Table 1. Specification of BLDC motor rating

Parameter	Value	Unit
Rated power	1.2	kW
Rated voltage	48	V
Rated speed	4500	RPM
Rated current	25	A
Back-EMF constant	0.102	V/(rad/s)
Torque constant	0.102	Nm/A
Armature resistance	0.05	Ω
Rotor inertia	0.005	kg·m²
Friction coefficient	0.0005	Nms

The chosen BLDC motor rating of 1.2 kW at 48 V is an excellent choice for a two-wheeler electric vehicle (EV) because of its balanced mix of power, efficiency, and safety. A 1.2 kW engine delivers enough power for all usual riding scenarios, such as rapid acceleration from a stop, maintaining stable cruising speeds, and successfully climbing inclines. This guarantees that the user has a dynamic and responsive riding experience. Moreover, the 48 V operating voltage is a widely accepted standard for light EVs because it strikes a critical balance: it's high enough to minimise current draw, reducing heat losses and allowing for a more compact and efficient battery pack design, while remaining within a low-voltage range that prioritises rider safety. As a result, this motor rating is a practical and acceptable choice that fulfils the real-world performance needs and design limits of a modern EV bike.

2.2. System modelling

The Landsman converter as shown in Figure 2, is a novel DC-DC converter architecture that combines the features of buck-boost and Cuk converters, resulting in a controlled DC output voltage with better performance. In electric vehicle (EV) drive applications, it is typically used to connect the rectified AC supply to the voltage source inverter (VSI) that powers the BLDC motor.

2.2.1. Input stage

The single-phase AC power supply is first filtered to eliminate high-frequency harmonics before being rectified using a bridgeless design. This eliminates the traditional diode bridge rectifier and decreases conduction losses, resulting in higher efficiency. The rectified DC is sent to the Landsman converter.

2.2.2. Energy storage and transfer

The converter uses two inductors, two capacitors, and controlled switches to store and transmit energy. During the switch-on state, the input inductor stores energy, while the capacitor sends energy to the load via the output inductor. During the switch OFF state, the inductor's stored energy is released via the diode, charging the intermediate capacitor and sending energy to the load. This dual energy-transfer system maintains continuous power flow while minimizing current ripples at both the input and output.

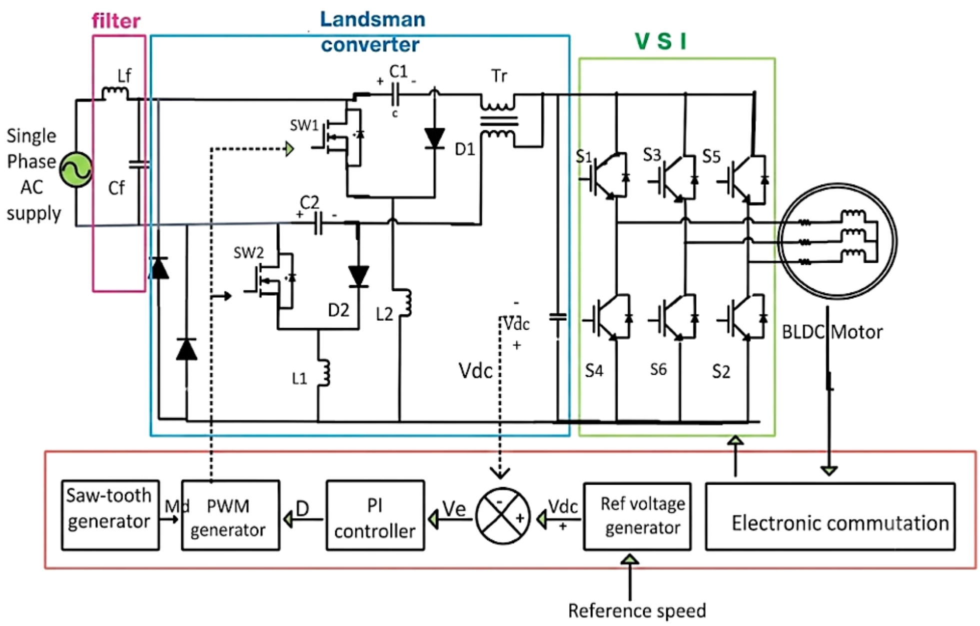

Figure 2. Design of Landsman converter

2.2.3. Voltage regulation

The Landsman converter's output DC voltage is regulated by adjusting the duty cycle of the switching devices. A closed-loop control approach, which usually employs a PI controller or intelligent control (such as fuzzy-based sliding mode), changes the duty ratio depending on the reference speed and voltage error. This assures that the BLDC motor receives a constant DC connection voltage, regardless of supply or load fluctuations.

2.2.4. Purpose of Landsman converter in BLDC motor drive for EV applications

The Landsman converter is a hybrid DC–DC topology that combines buck and boost characteristics, making it suitable for electric two-wheeler BLDC motor drives. It supplies a regulated DC-link voltage to the voltage source inverter (VSI), ensuring stable motor performance under varying supply and battery conditions. The converter also reduces switching stress, improving efficiency and reliability, and supports bidirectional power flow for regenerative braking, thereby enhancing driving range [12]-[14]. Despite a higher component count, it offers advantages such as improved DC-link voltage regulation, reduced input current ripple, and inherent power factor correction when interfaced with an AC source. It also provides better voltage gain and dynamic performance. Additionally, its high efficiency, reduced harmonic distortion, and precise duty cycle control enable accurate speed regulation and suitability for grid-connected operation. Overall, it serves as a compact, efficient, and reliable solution for modern EV applications [15], [16].

2.2.5. Controller for converter

In electric two-wheeler applications, effective Landsman converter control is essential for maintaining BLDC motor speed and DC-link voltage. A PI controller is commonly used due to its simplicity, generating the duty cycle based on speed error. The proportional term ensures fast response, while the integral term eliminates steady-state error. However, its performance degrades under sudden load variations and parameter uncertainties typical of EV operation. To overcome these limitations, a fuzzy sliding mode controller (FSMC) is employed. It combines the robustness of sliding mode control with the adaptive capability of fuzzy logic, enabling improved transient response, reduced chattering, and accurate speed tracking under varying conditions. As a result, the FSMC-based system offers enhanced efficiency, stability, and reliability compared to conventional PI control, making it well suited for EV applications.

2.3. Design of Landsman converter

The Landsman converter's specifications depend on the BLDC motor ratings and the intended DC-link voltage. The Landsman converter for driving a BLDC motor in two-wheeler EV applications is designed around the motor's rated needs and the peculiarities of the input AC supply [17]. The converter is powered by a single-phase AC supply of 230 V RMS, 50 Hz, which, after rectification, produces a peak voltage of roughly 325 volts. To ensure the BLDC motor's steady functioning, the converter sets the DC-link voltage to 48 V, which matches the motor's rated needs. With the motor rated at 1.2 kW, the converter must be able to produce the required power while retaining efficiency and voltage stability. A 50 kHz switching frequency with a 20 µs period balances dynamic responsiveness, switching losses, and filter size. Because the converter runs in boost mode to increase voltage under low input circumstances, the maximum duty cycle is set at 0.8, ensuring enough voltage gain while minimizing instability [9]. This specification framework sets the Landsman converter's operational limitations and provides consistent performance under changing supply and load situations.

2.3.1. Inductor design

To maintain a constant current and avoid discontinuous operation, which might result in increased voltage stress, the inductors must be big enough to function in continuous conduction mode (CCM). The minimum inductance for CCM is determined to guarantee that the inductor current never reaches zero.
- Average inductor current (IL): The inductors must be able to handle at least the full-load current of 25 A.
- Ripple current (ΔI_L): To maintain CCM, we allow for a 20% ripple current relative to the average current.

$$\Delta IL = 0.20 \cdot IL\_avg \approx 0.20 \cdot 25\, A = 5\, A$$

Minimum inductance for the forward (boost) mode: The minimum inductance (L min) is determined to keep the inductor current from going below zero. Here's (1).

$$L_{min} = \frac{V_{in} . D_{max}}{2 . \Delta I_L . f_{sw}} \quad (1)$$

For boost mode, the required duty cycle (D) is (2).

$$D = 1 - \frac{V_{in}}{V_{out}} \quad (2)$$

The worst case occurs at the lowest battery voltage, $Vin = 42\, V$

$$D = 1 - \frac{42}{48} = 0.125$$

$$L_{min} = \frac{42\ V\ .0.125}{5A.50.10^3\ Hz} = 21\ \mu H$$

To ensure a safety margin, we choose a standard value that is at least twice the lowest calculated value. Hence, the selected value: $L1 = L2 = 100\ \mu H$.

2.3.2. Capacitor design

The capacitors C1 and C2 are important to the converter's bridgeless operation. They are charged to the maximum voltage of the AC source. For a 230 V RMS source, the peak voltage is $Vpeak = 230\sqrt{2} \approx 325\ V$.

- Ripple voltage (ΔV_C): We design for a maximum ripple voltage of 5% of the peak voltage across the capacitor, which is $0.05 \times 325\ V\ \approx 16.25\ V$.
- Ripple current: The ripple current equals the average input current to the converter, which is about the motor's rated current. I = 25 A.
- Capacitance (C): The capacitance is designed to accommodate the ripple current during a single switching period.

$$C = \frac{I_{rated}}{\Delta V_C . f_{sw}} \tag{3}$$

$$C = \frac{25A}{50*10^3 Hz*16.25\ V} = 30.7\ \mu F$$

A standard robust value is selected for both capacitors.

$$C1 = C2 = 47\ \mu F$$

2.3.3. DC link and input capacitor design

The capacitors must handle this voltage and the ripple current associated with the energy transfer. The capacitors filter out voltage ripple and stabilize the DC bus voltage. We design them to maintain the ripple voltage to a reasonable level, usually 1% of the nominal voltage.

- Output capacitor (C_{out}): This capacitor stabilizes the 48 V DC bus for the motor.

$$C_{out} = \frac{I_{out} . D\ max}{\Delta V_{out} . f_{sw}} \tag{4}$$

Assuming a maximum duty cycle of D_{max} = 0.8 (for boost operation) and a ripple voltage (ΔV_{out}) of 1% of 48 V, which is 0.48 V.

$$C_{out} = \frac{25A*0.8}{50*10^3 Hz*0.48\ V} = 667\ \mu F$$

To be safe, we choose a standard value higher than this. Hence, the selected value of the output capacitor is,

$$Cout = 1000\ \mu F$$

- Input capacitor (C in): This capacitor filters the ripple from the input AC source. Hence, the selected value of the input capacitor is, $Cin = 220\ \mu F$.

2.3.4. Switch selection

The switches (SW_1 and SW_2) and diodes (D_1 and D_2) must have appropriate voltage and current ratings to handle the stresses during operation.

- Voltage rating: The switches must withstand a voltage greater than the maximum DC link voltage of 48 V. Hence, a safety margin is essential, and the selected voltage rating should be greater than 60 V
- Current rating: The switches must be able to carry the full-load current of 25 A plus the ripple current. Hence, the selected current rating should be greater than 30 A.

The ratings of the designed components of the Landsman converter are shown in Table 2.

Table 2. Specification of Landsman converter

Component	Selected value
Inductors (L1, L2)	100 μH
Capacitors (C1, C2)	47 μF
Input capacitor (Cin)	220 μF
Output capacitor (C_{out})	1000 μF
Switches (SW1, SW2)	Rated > 60 V, > 30 A
Switching frequency (fsw)	50 Hz

3. DESIGN OF CONTROLLER

In order to ensure steady and precise functioning under all circumstances, the controller is essential in controlling the speed of a BLDC motor powered by a Landsman converter. By continuously comparing the reference and real speeds and modifying the converter's power flow accordingly, it maintains the intended motor speed. A cascaded control structure is used to do this, with the inner loop controlling the DC-link voltage and the outer loop controlling speed. Additionally, the controller allows for efficient rejection of disturbances like load fluctuations, guaranteeing minimal degradation and smooth operation. In general, it maintains power quality while improving system robustness, responsiveness, and efficiency [12]. The PI and FSMC controllers of a BLDC motor drive manage the motor's speed and guarantee that its performance stays steady under different operating circumstances. While they have the same goal, they do it via various control mechanisms, which results in diverse performance characteristics.

3.1. PI controller

The proportional–integral (PI) controller is used to regulate BLDC motor speed by minimizing the error between reference and actual values. The proportional term (K_p) provides an immediate response to speed error, enabling fast correction, while the integral term (K_i) eliminates steady-state error to ensure accurate tracking. This structure offers a simple and reliable control strategy, though its performance may degrade under nonlinearities and sudden disturbances.

A cascaded control approach is employed, consisting of an outer speed loop and an inner voltage loop. The speed error is defined as (5).

$$e_{speed}(t) = N_{ref} - N_{actual}(t) \tag{5}$$

The corresponding controller output, which acts as the reference voltage (V_{ref}), is given by (6).

$$u_{speed}(t) = Kp_{speed} \cdot e_{speed}(t) + Ki_{speed} \int e_{speed}(t) \tag{6}$$

In the inner loop, the DC-link voltage error is calculated as (7).

$$e_{voltage}(t) = V_{ref} - V_{dc\_actual}(t) \tag{7}$$

The PI controller then generates the duty cycle for the Landsman converter as (8).

$$D(t) = Kp_{voltage} \cdot e_{voltage}(t) + Ki_{voltage} \int e_{voltage}(t)dt \tag{8}$$

This cascaded PI structure ensures effective speed regulation by coordinating voltage control and motor dynamics.

3.2. Fuzzy based sliding mode control

The sliding mode control (SMC) is a robust nonlinear technique that drives the system state to a predefined sliding surface and maintains it there, ensuring strong disturbance rejection and robustness against uncertainties [17]-[20]. It operates in two phases: a reaching phase that forces the state to the surface using high-gain control, and a sliding phase that ensures convergence to equilibrium. However, conventional SMC suffers from chattering due to high-frequency switching. To mitigate this, a fuzzy sliding mode controller (FSMC) is employed, where fuzzy logic adaptively adjusts the switching gain, reducing chattering while retaining robustness. The sliding surface is defined as (9).

$$S = \lambda \cdot e_{speed} + \int e_{speed} dt \tag{9}$$

Where λ is weighting constant.

A Mamdani-type fuzzy inference system (FIS) uses S and Ṡ as inputs to generate adaptive gain K. The triangular membership functions with seven linguistic variables (NB to PB) form a 49-rule base, ensuring effective control across operating conditions. The control law combines equivalent and switching components (10).

$$V_{sw} = -Kf * sign(S) \quad (10)$$

The equivalent control is expressed as (11).

$$V_{eq} = \frac{1}{\lambda}\dot{V}ref \quad (11)$$

The final control output:

$$V_{ref} = V_{eq} + V_{sw} \quad (12)$$

Figure 3 presents the rule-base surface generated by the fuzzy inference system, and the complete set of 49 fuzzy rules used to determine the adaptive switching gain is listed in Table 3.

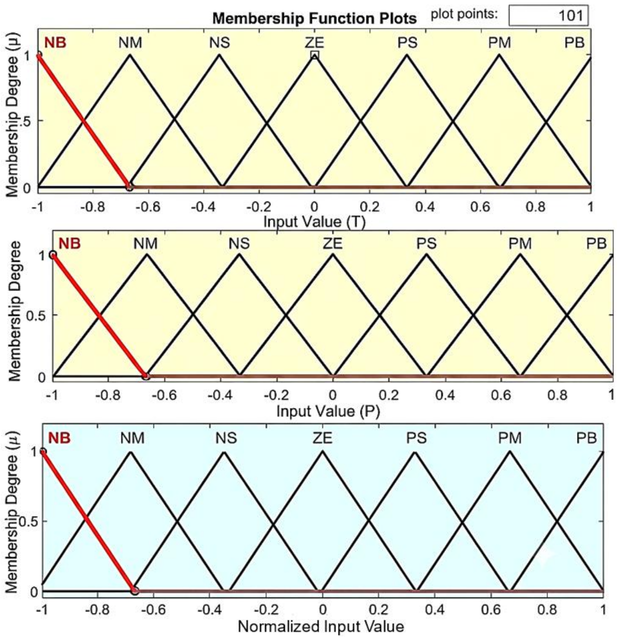

Figure 3. Rule base of the FIS

Table 3. Fuzzy rule base

$S \setminus \dot{S}$	NB	NM	NS	Z	PS	PM	PB
NB	PB	PB	PB	PM	PM	PS	Z
NM	PB	PB	PM	PM	PS	Z	NS
NS	PB	PM	PM	PS	Z	NS	NM
Z	PM	PM	PS	Z	NS	NM	NM
PS	PM	PS	Z	NS	NM	NM	NB
PM	PS	Z	NS	NM	NM	NB	NB
PB	Z	NS	NM	NM	NB	NB	NB

4. PROPOSED SYSTEM

The suggested BLDC motor drive system is intended for electric two-wheeler applications and operates on a single-phase 230 V, 50 Hz AC supply. The input AC is rectified and fed into a bridgeless Landsman converter, which assures effective DC-DC conversion and provides a regulated 48 V DC-link voltage sufficient for the BLDC motor drive. The converter switches at a frequency of 50 kHz, and its duty cycle is modified to maintain a steady voltage under changing load and input circumstances. The regulated DC output from the converter is sent into the voltage source inverter (VSI), which generates electronically commutated signals to power the BLDC motor. This arrangement guarantees better voltage control, lower ripple content, and dependable performance of the motor drive system.

A closed-loop feedback system that continuously compares the actual speed with the reference to produce an error signal is used to control the BLDC motor speed. Either a PI controller or a fuzzy sliding mode controller (FSMC) handles this problem. The FSMC improves dynamic responsiveness through adaptive tuning and durability, while the PI controller guarantees good steady-state performance. To maintain the intended speed, the controller output modifies the converter duty cycle using the reference voltage. Motor speed, torque, and DC-link voltage are used to assess system performance. The simulation parameters and component ratings adopted for the MATLAB/Simulink model are summarized in Table 4.

Table 4. Simulation parameters and component ratings

Parameter	Values
DC input voltage vin	48 V
Rated power (BLDC motor) P	1.2 kW
Switching frequency fsw	50 kHz
Landsman inductors L1, L2	450 µH, 500 µH
Intermediate capacitor C1	10 µF
Filter capacitor C2	2200 µF
Stator resistance RS	0.18 Ω
Stator inductance LS	0.45 mH
Torque constant KT	0.55 Nm/A

The MATLAB/Simulink environment was used to create the model in Figure 4, which depicts a full AC-fed BLDC motor drive with integrated power conversion and closed-loop control. The Landsman converter's switching transients are precisely captured by an ODE4 (Runge-Kutta) solver with a fixed step size of 1×10−6 s, and the FSMC is constructed using an S-Function to minimize computational time. Table 4 lists important metrics and ratings. Both controllers accomplish adequate speed regulation, according to simulation data, but the FSMC performs better in terms of quicker dynamic response, better disturbance rejection, and more seamless reference tracking. A diode bridge rectifier is used to convert the system's 230 V, 50 Hz AC supply to DC after it has been conditioned by an LC filter and transformer. A Landsman converter controls this DC to keep the DC-link steady under a variety of circumstances. A three-phase voltage source inverter receives the regulated output and uses gate signals synchronized with rotor position from Hall sensors to operate the BLDC motor. Accurate performance evaluation is made possible by the motor operating under actual load circumstances. In order to provide an error signal, a closed-loop control approach is used in which the actual motor speed is continuously compared with the reference. To achieve the required dynamic performance, the PI or FSMC controller modifies the DC–DC converter duty cycle and inverter switching based on this inaccuracy.

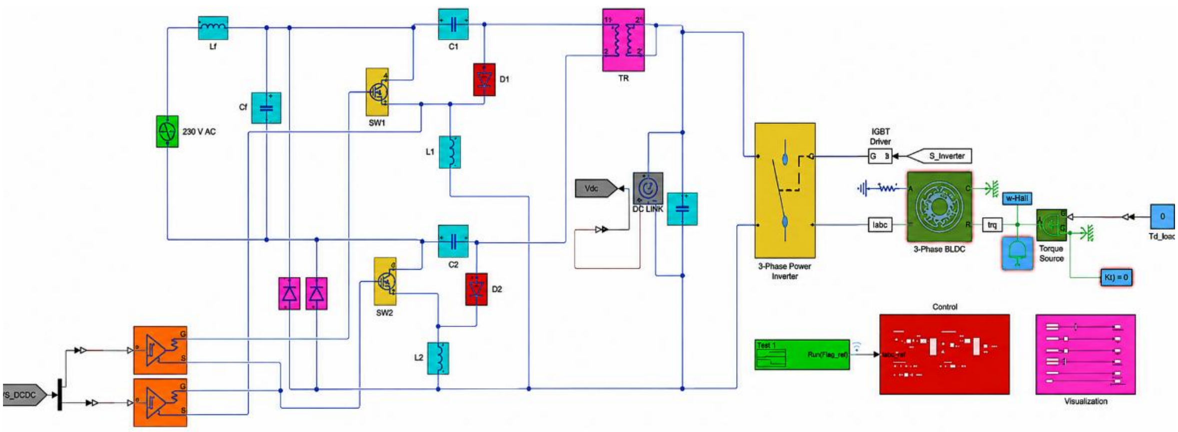

Figure 4. Simulink model of speed control of BLDC motor with controller

The fuzzy controller balances computational efficiency and sensitivity by using seven triangle membership functions with error (e) and change in error (Δe) as inputs. In order to minimize chattering, the rule base guarantees low gain close to steady state and strong control gain during significant mistakes. This makes it possible to effectively control voltage, torque, and speed in both transient and steady-state situations. Important metrics like motor speed, electromagnetic torque, stator current, and DC-link voltage are used to track system performance.

5. SIMULATION RESULTS

The simulation results give a comprehensive comparison of the proportional-integral (PI) controller and the fuzzy sliding mode controller (FSMC) for controlling the speed of the BLDC motor. The examination focuses on various performance aspects such as transient response, dynamic and steady state response, reaction during starting and the system's capacity to withstand a severe load disruption. As illustrated in Figure 5, the Landsman converter rectifies and regulates a 230 V AC supply to maintain a 48 V DC-link voltage for both controllers, guaranteeing the power stage operates as intended. The FSMC has a more stable voltage profile, suggesting better control performance, even if both controllers reach the set point.

5.1. Transient response

The transient response shown in Figure 6 assesses the motor's behavior from the moment a command is initiated until it stabilizes at the target speed of 4500 RPM. As summarized in Table 5, the FSMC outperforms the PI controller on all major performance indicators. The FSMC demonstrates a notably faster rise time of 0.064 seconds versus 0.180 seconds for the PI controller, reflecting a more responsive system. It also achieves a minimal overshoot of 0.17%, ensuring a smooth and accurate approach to the setpoint, while the PI controller exhibits a higher overshoot of 2.13%, causing oscillations. Additionally, the FSMC reaches steady-state at the desired speed within 0.212 seconds, significantly quicker than the PI controller's 0.622 seconds. This enhanced transient performance results from the FSMC's adaptive control gain, which allows rapid convergence to the setpoint while minimizing excessive oscillations.

Table 5. Transient response characteristics

Specification	PI controller	Fuzzy SMC
Rise time (s)	0.180	0.064
Overshoot (%)	2.13	0.17
Settling time (s)	0.622	0.212

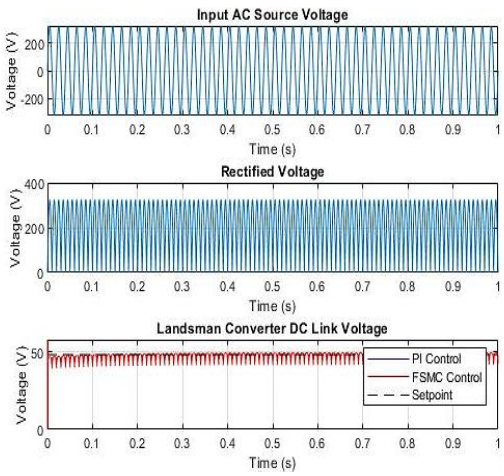

Figure 5. Simulink results of input characteristics

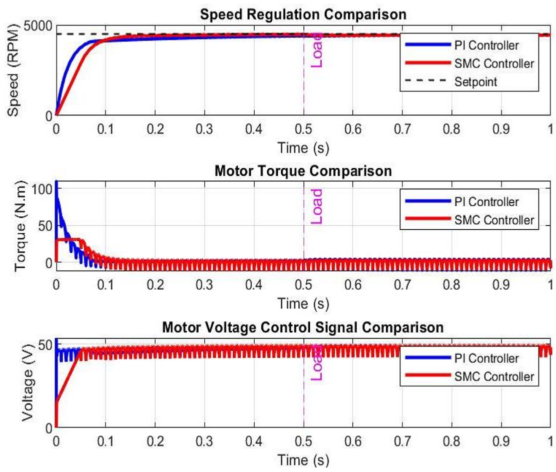

Figure 6. Simulink results of comparison of output characteristics for PI and FSMC controller

5.2. Dynamic response and steady state response

Figure 7 illustrates that the FSMC controller significantly outperforms the PI controller in both dynamic response and steady-state performance. In the torque–speed characteristics, the PI controller displays large fluctuations during startup, with torque exceeding 100 Nm, reflecting an aggressive and less controlled response. Conversely, the FSMC delivers a smoother and more stable torque profile, quickly reaching steady-state operation with minimal variation. This leads to better transient handling and more consistent performance, particularly under load conditions. When a load is applied at t = 0.5 seconds, the FSMC exhibits only a slight deviation and recovers almost immediately, while the PI controller reacts more slowly and shows noticeable oscillations. The torque–current relationship confirms the fundamental proportionality (T = KT * Ia), with both controllers displaying a linear trend, thereby validating the motor model. However, the FSMC produces a clean and consistent linear curve, reflecting precise current control, while the PI controller exhibits greater dispersion, especially during high-current transient events. Regarding the speed–current characteristics, the PI controller experiences a large inrush current exceeding 1000 A during startup, indicating an aggressive and less optimized response. In contrast, the FSMC limits the peak current to approximately 200 A, enabling a smoother and more efficient startup. This reduction in current stress enhances system reliability and overall control performance.

5.3. Load disturbance rejection performance

The load disturbance test (Figure 6) assesses the controller's capability to maintain motor speed when a sudden torque of 1.0 Nm is applied at t = 0.5 seconds during operation at 4500 RPM. As detailed in Table 6, the FSMC demonstrates superior resilience. The PI controller experiences a speed drop of 185 RPM, whereas the FSMC limits the drop to just 45 RPM, indicating better disturbance rejection. Additionally, the FSMC restores speed to the setpoint within 0.04 seconds, significantly faster than the PI controller's 0.16-second recovery time (s). This underscores the FSMC's adaptability and effectiveness in handling sudden load changes. Figure 8 further illustrates that the FSMC produces lower current and torque ripple compared to the PI controller. By replacing the abrupt switching characteristic of conventional SMC with a smooth fuzzy-based control action, the FSMC effectively reduces chattering while maintaining robust performance. Practically speaking, standard power electronic components and inexpensive digital controllers such as DSPs or microcontrollers can be used to implement the suggested control technique [21]-[27].

Table 6. Load disturbance response characteristics

Specification	PI controller	Fuzzy SMC
Speed drop (RPM)	185	45
Recovery time	0.16	0.04

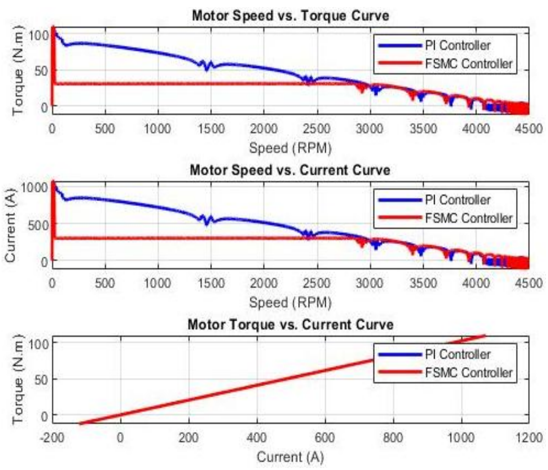

Figure 7. Simulink results of dynamic response

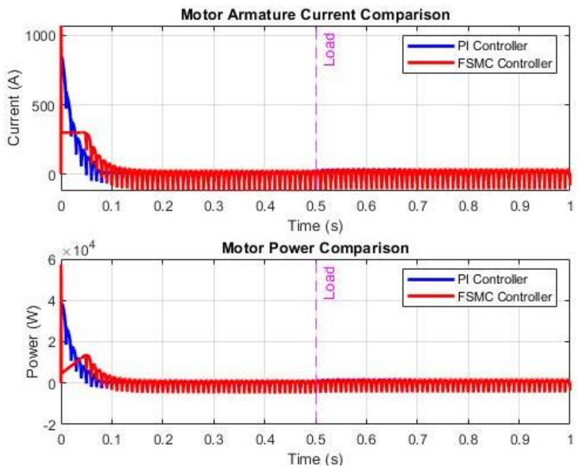

Figure 8. Simulink results of current and power

6. CONCLUSION

This research compares the speed control of BLDC motor powered by a Landsman DC-DC converter using PI and fuzzy-based sliding mode controllers. According to simulation studies, the fixed-gain construction of the PI controller causes poorer transient response and less robustness under load disturbances, even though it offers respectable steady-state performance. The FSMC, on the other hand, performs better dynamically, as seen by its quicker rise time, reduced overshoot, quicker settling time, and improved disturbance rejection.

The FSMC's adaptability enables it to successfully lower chattering while preserving the sliding mode control's intrinsic resilience. In order to provide a steady DC-link voltage and enhance overall system performance, the Landsman converter is essential. In order to evaluate real-time performance, switching losses, and thermal behavior under realistic operating settings, future work will concentrate on experimental validation.

FUNDING INFORMATION

The authors state that no funding was involved in this work.

AUTHOR CONTRIBUTIONS STATEMENT

This journal uses the Contributor Roles Taxonomy (CRediT) to recognize individual author contributions, reduce authorship disputes, and facilitate collaboration.

Name of Author	C	M	So	Va	Fo	I	R	D	O	E	Vi	Su	P	Fu
S. Sahana	✓	✓	✓	✓	✓	✓			✓					
K. Sasikala	✓						✓			✓		✓	✓	

C : **C**onceptualization	I : **I**nvestigation	Vi : **Vi**sualization
M : **M**ethodology	R : **R**esources	Su : **Su**pervision
So : **So**ftware	D : **D**ata Curation	P : **P**roject administration
Va : **Va**lidation	O : Writing - **O**riginal Draft	Fu : **Fu**nding acquisition
Fo : **Fo**rmal analysis	E : Writing - Review & **E**diting	

CONFLICT OF INTEREST STATEMENT

The authors declare that they have no known competing financial interests or personal relationships that could have appeared to influence the work reported in this paper. The authors state no conflict of interest.

DATA AVAILABILITY

The data that support the findings of this study are available from the corresponding author upon reasonable request.

REFERENCES

[1] C. Liu, K. T. Chau, C. H. T. Lee, and Z. Song, "A critical review of advanced electric machines and control strategies for electric vehicles," *Proceedings of the IEEE*, vol. 109, no. 6, pp. 1004–1028, Jun. 2021, doi: 10.1109/JPROC.2020.3041417.

[2] A. Emadi, Y. J. Lee, and K. Rajashekara, "Power electronics and motor drives in electric, hybrid electric, and plug-in hybrid electric vehicles," *IEEE Transactions on Industrial Electronics*, vol. 55, no. 6, pp. 2237–2245, Jun. 2008, doi: 10.1109/TIE.2008.922768.

[3] K. T. Chau, C. C. Chan, and C. Liu, "Overview of permanent-magnet brushless drives for electric and hybrid electric vehicles," *IEEE Transactions on Industrial Electronics*, vol. 55, no. 6, pp. 2246–2257, Jun. 2008, doi: 10.1109/TIE.2008.918403.

[4] J. J. Eckert, L. C. A. Silva, E. S. Costa, F. M. Santiciolli, F. G. Dedini, and F. C. Corrêa, "Electric vehicle drivetrain optimisation," *IET Electrical Systems in Transportation*, vol. 7, no. 1, pp. 32–40, Mar. 2017, doi: 10.1049/iet-est.2016.0022.

[5] J. Shao, D. Nolan, M. Teissier, and D. Swanson, "A novel microcontroller-based sensorless brushless DC (BLDC) motor drive for automotive fuel pumps," *IEEE Transactions on Industry Applications*, vol. 39, no. 6, pp. 1734–1740, Nov. 2003, doi: 10.1109/TIA.2003.818973.

[6] V. Kumarasamy, V. K. T. Ramasamy, G. Chandrasekaran, G. Chinnaraj, P. Sivalingam, and N. S. Kumar, "A review of integer order PID and fractional order PID controllers using optimization techniques for speed control of brushless DC motor drive," *International Journal of System Assurance Engineering and Management*, vol. 14, no. 4, pp. 1139–1150, Aug. 2023, doi: 10.1007/s13198-023-01952-x.

[7] A. S. El-Wakeel, A. E.-E. K. M. Ellissy, and A. M. Abdel-Hamed, "A hybrid bacterial foraging-particle swarm optimization technique for optimal tuning of proportional-integral-derivative controller of a permanent magnet brushless DC motor," *Electric Power Components and Systems*, vol. 43, no. 3, pp. 309–319, Feb. 2015, doi: 10.1080/15325008.2014.981320.

[8] K. Vanchinathan and K. R. Valluvan, "A metaheuristic optimization approach for tuning of fractional-order PID controller for speed control of sensorless BLDC motor," *Journal of Circuits, Systems and Computers*, vol. 27, no. 08, p. 1850123, Jul. 2018, doi: 10.1142/S0218126618501232.

[9] J. Feng, "Parameter fuzzy rectification for sliding mode control of five-phase permanent magnet synchronous motor speed control system," *Frontiers in Mechanical Engineering*, vol. 10, Jul. 2024, doi: 10.3389/fmech.2024.1391593.

[10] X. Kong, Z. Deng, Y. Zhao, and W. Gao, "Stability control of distributed drive electric vehicle based on adaptive fuzzy sliding mode," *Proceedings of the Institution of Mechanical Engineers, Part D: Journal of Automobile Engineering*, vol. 238, no. 9, pp. 2741–2752, Aug. 2024, doi: 10.1177/09544070231169804.

[11] H. Niu, J. Yu, H. Yu, C. Lin, and L. Zhao, "Adaptive fuzzy output feedback and command filtering error compensation control for permanent magnet synchronous motors in electric vehicle drive systems," *Journal of the Franklin Institute*, vol. 354, no. 15, pp. 6610–6629, Oct. 2017, doi: 10.1016/j.jfranklin.2017.08.021.

[12] P. K. Singh, B. Singh, V. Bist, K. Al-Haddad, and A. Chandra, "BLDC motor drive based on bridgeless landsman PFC converter with single sensor and reduced stress on power devices," *IEEE Transactions on Industry Applications*, vol. 54, no. 1, pp. 625–635, Jan. 2018, doi: 10.1109/TIA.2017.2740281.

[13] B. Singh and R. Kumar, "Solar photovoltaic array fed water pump driven by brushless DC motor using landsman converter," *IET Renewable Power Generation*, vol. 10, no. 4, pp. 474–484, Apr. 2016, doi: 10.1049/iet-rpg.2015.0295.

[14] N. S. Kumar *et al.*, "A novel design methodology and numerical simulation of BLDC motor for power loss reduction," *Applied Sciences*, vol. 12, no. 20, p. 10596, Oct. 2022, doi: 10.3390/app122010596.

[15] V. Bist and B. Singh, “A reduced sensor PFC BL-zeta converter-based VSI-fed BLDC motor drive,” *Electric Power Systems Research*, vol. 98, pp. 11–18, May 2013, doi: 10.1016/j.epsr.2013.01.006.

[16] V. Bist and B. Singh, “An adjustable-speed PFC bridgeless buck–boost converter-fed BLDC motor drive,” *IEEE Transactions on Industrial Electronics*, vol. 61, no. 6, pp. 2665–2677, Jun. 2014, doi: 10.1109/TIE.2013.2274424.

[17] K. Premkumar and B. V. Manikandan, “Adaptive neuro-fuzzy inference system based speed controller for brushless DC motor,” *Neurocomputing*, vol. 138, pp. 260–270, Aug. 2014, doi: 10.1016/j.neucom.2014.01.038.

[18] R. Shenbagalakshmi, S. K. Mittal, J. Subramaniyan, V. Vengatesan, D. Manikandan, and K. Ramaswamy, “Adaptive speed control of BLDC motors for enhanced electric vehicle performance using fuzzy logic,” *Scientific Reports*, vol. 15, no. 1, p. 12579, Apr. 2025, doi: 10.1038/s41598-025-90957-6.

[19] C. Wang and Z. Q. Zhu, “Fuzzy logic speed control of permanent magnet synchronous machine and feedback voltage ripple reduction in flux-weakening operation region,” *IEEE Transactions on Industry Applications*, vol. 56, no. 2, pp. 1505–1517, Mar. 2020, doi: 10.1109/TIA.2020.2967673.

[20] J. Zhang, J. Sun, H. Gu, H. Poloei, and A. Karami, “Control of PMSM chaos using backstepping-based adaptive fuzzy method in the presence of uncertainty and disturbance,” *Systems Science and Control Engineering*, vol. 9, no. 1, pp. 673–688, Jan. 2021, doi: 10.1080/21642583.2021.1980130.

[21] A. Sathyan, N. Milivojevic, Young-Joo Lee, M. Krishnamurthy, and A. Emadi, “An FPGA-based novel digital PWM control scheme for BLDC motor drives,” *IEEE Transactions on Industrial Electronics*, vol. 56, no. 8, pp. 3040–3049, Aug. 2009, doi: 10.1109/TIE.2009.2022067.

[22] M. A. Awadallah, M. M. Morcos, S. Gopalakrishnan, and T. W. Nehl, “A neuro-fuzzy approach to automatic diagnosis and location of stator inter-turn faults in CSI-fed PM brushless DC motors,” *IEEE Transactions on Energy Conversion*, vol. 20, no. 2, pp. 253–259, Jun. 2005, doi: 10.1109/TEC.2005.847976.

[23] M. A. Salvador, T. B. Lazzarin, and R. F. Coelho, “High step-up DC–DC converter with active switched-inductor and passive switched-capacitor networks,” *IEEE Transactions on Industrial Electronics*, vol. 65, no. 7, pp. 5644–5654, Jul. 2018, doi: 10.1109/TIE.2017.2782239.

[24] A. Murali, R. S. Wahab, C. S. R. Gade, C. Annamalai, and U. Subramaniam, “Assessing finite control set model predictive speed controlled PMSM performance for deployment in electric vehicles,” *World Electric Vehicle Journal*, vol. 12, no. 1, p. 41, Mar. 2021, doi: 10.3390/wevj12010041.

[25] R. G. Shriwastava, M. P. Thakare, K. V. Bhadane, M. S. Harne, and N. B. Wagh, “Performance enhancement of DCMLI fed DTC-PMSM drive in electric vehicle,” *Bulletin of Electrical Engineering and Informatics*, vol. 11, no. 4, pp. 1867–1881, Aug. 2022, doi: 10.11591/eei.v11i4.3714.

[26] A. Katkout, T. Nasser, and A. Essadki, “Robust multiobjective model predictive control with computation delay compensation for electric vehicle applications using PMSM with multilevel inverter,” *Mathematical Problems in Engineering*, vol. 2020, pp. 1–12, May 2020, doi: 10.1155/2020/7015865.

[27] M. S. Bhaskar, M. Meraj, A. Iqbal, S. Padmanaban, P. Kiran Maroti, and R. Alammari, “High gain transformer-less double-duty-triple-mode DC/DC converter for dc microgrid,” *IEEE Access*, vol. 7, pp. 36353–36370, 2019, doi: 10.1109/ACCESS.2019.2902440.

BIOGRAPHIES OF AUTHORS

S. Sahana is working as an assistant professor in the Department of Electrical and Electronics Engineering, Velammal Institute of Technology, Chennai, India. She received her Bachelor of Engineering from Jayasuriya Engineering College, Chennai, India, and Master of Engineering from Gojan School of Business and Technology, Chennai, India. She is pursuing her doctorate in electrical and electronic engineering as a research scholar at Vels Institute of Science, Technology and Advanced Studies, Chennai. She has published a paper in an IEEE Scopus-indexed conference. Her areas of interest include embedded systems, power electronics and drives, and new trending technologies. She can be contacted at email: sahana.mee05@gmail.com.

Dr. K. Sasikala is working as an associate professor in the Department of Electrical and Electronics Engineering, Vels Institute of Science Technology and Advanced Studies, Chennai. She received her Bachelor of Engineering from Bharathiyar University, Coimbatore, and Master of Engineering from Anna University, Chennai. She received her doctorate from Vels Institute of Science, Technology and Advanced Studies, Chennai. She has published more than 35 articles in Scopus, SCI, and UGC-approved journals. She has authored three books and five book chapters. She has filed and published seven utility patents and received grants for four design patents. Her areas of interest include power electronics, embedded systems, and renewable energy. She can be contacted at email: skala.se@vistas.ac.in.